JCB Article

Defective flagellar assembly and length regulation in *LF3* null mutants in *Chlamydomonas*

Lai-Wa Tam,[1] William L. Dentler,[2] and Paul A. Lefebvre[1]

[1]Department of Plant Biology, University of Minnesota, St. Paul, MN 55108
[2]Department of Molecular Biosciences, University of Kansas, Lawrence, KS 66045

Four long-flagella (*LF*) genes are important for flagellar length control in *Chlamydomonas reinhardtii*. Here, we characterize two new null *lf3* mutants whose phenotypes are different from previously identified *lf3* mutants. These null mutants have unequal-length flagella that assemble more slowly than wild-type flagella, though their flagella can also reach abnormally long lengths. Prominent bulges are found at the distal ends of short, long, and regenerating flagella of these mutants. Analysis of the flagella by electron and immunofluorescence microscopy and by Western blots revealed that the bulges contain intraflagellar transport complexes, a defect reported previously (for review see Cole, D.G., 2003. *Traffic*. 4:435–442) in a subset of mutants defective in intraflagellar transport. We have cloned the wild-type *LF3* gene and characterized a hypomorphic mutant allele of *LF3*. LF3p is a novel protein located predominantly in the cell body. It cosediments with the product of the *LF1* gene in sucrose density gradients, indicating that these proteins may form a functional complex to regulate flagellar length and assembly.

Introduction

A cell is capable of regulating its own size and the size of its organelles to achieve a particular differentiated state. Eukaryotic cilia and flagella are particularly interesting because they are present in many types of tissues and organisms and are important for sensory functions, cell motility, molecular transport, and the establishment of left–right asymmetry in vertebrates. Optimal lengths of these organelles are crucial for carrying out their diverse cellular functions. In humans, abnormally long flagella are associated with primary ciliary dyskinesia (Afzelius et al., 1985; Niggemann et al., 1992) and extra short cilia cause impaired mucociliary function (Rautiainen et al., 1991). Understanding mechanisms that regulate flagellar length should provide insights into the regulation of microtubule growth and dynamics because doublet and single microtubules are the main structural components of flagella.

Chlamydomonas reinhardtii provides an ideal experimental system for studying flagellar length control because of its tight regulation of flagellar length. Each *Chlamydomonas* cell has two equal-length flagella, and the length of the flagella falls within a very narrow range of values in a population of cells. When flagella are amputated, *Chlamydomonas* cells can sense the loss and regrow their flagella rapidly to the predeflagellation lengths within 90 min (Rosenbaum et al., 1969). *Chlamydomonas* cells maintain two equal-length flagella. If one flagellum is amputated, then the remaining one shortens as a new one grows. When the two flagella reach the same length, they grow at the same rate to the predeflagellation length (Rosenbaum et al., 1969).

A number of genetic loci that affect flagellar length have been identified. Mutations in four long-flagella genes, *LF1*, *LF2*, *LF3*, and *LF4*, produce flagella of two to three times the normal length (McVittie, 1972; Barsel et al., 1988; Asleson and Lefebvre, 1998). Mutations in three short-flagella genes, *SHF1*, *SHF2*, and *SHF3*, produce half-length flagella (Jarvik et al., 1984; Kuchka and Jarvik, 1987). Dikaryon rescue experiments provide evidence for the dynamic nature of flagellar length regulation. When an *lf* mutant is mated to a wild-type (WT) cell, the cells fuse to form a temporary quadriflagellated cell (a dikaryon) with two long and two normal-length flagella. Within minutes, the long flagella shorten to WT length, whereas the normal-length flagella remain unchanged (Barsel et al., 1988). When short-flagella mutants are mated to WT cells, the short flagella rapidly grow to normal lengths (Jarvik et al., 1984). These results demonstrate that the

Address correspondence to Paul A. Lefebvre, Dept. of Plant Biology, University of Minnesota, 250 Biological Sciences Center, 1445 Gortner Ave., St. Paul, MN 55108. Tel.: (612) 624-0729. Fax: (612) 625-1738. email: pete@biosci.cbs.umn.edu

Key words: cilia; intraflagellar transport; organelle size control; unequal-length flagella

Abbreviations used in this paper: DIC, differential interference contrast; IFT, intraflagellar transport; Ulf, unequal-length flagella; WT, wild-type.

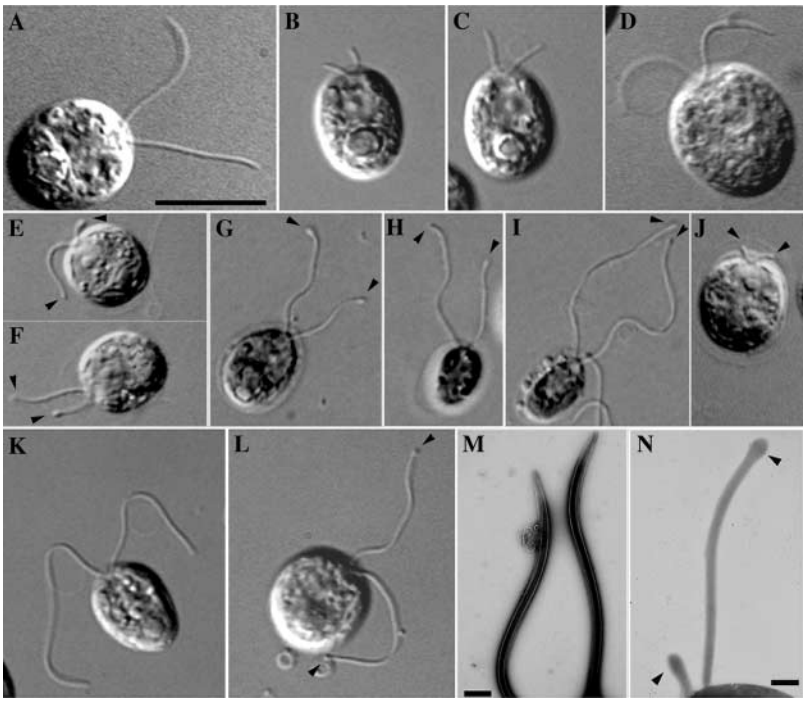

Figure 1. **Flagellar defects in Ulf and *lf3-2* mutants.** DIC images of WT cells with (A) fully grown flagella or with (B–D) intermediate-length flagella undergoing regeneration after deflagellation reveal that they have two equal-length flagella. In contrast, Ulf1 (*lf3-5*) cells possess (E–I) two flagella that are unequal in length. In a population of Ulf1 cells, the length of the flagella varies greatly, from (H and I) abnormally long flagella to (J) very short or stumpy flagella. In the (K and L) *lf3-2* mutant, most cells possess extra-long flagella, some of which show distal swellings (arrowheads). The distal tips of WT flagella are blunt or tapered, as viewed by (A–D) DIC or by transmission EM of negatively stained whole cell mounts (M), but the tips of all Ulf1 flagella, regardless of length, are bulged (E–J and N, arrowheads). The Ulf3 (*lf3-6*) mutant has phenotypes identical to those of the Ulf1 mutant. Bars: (DIC images) 10 μm; (electron micrographs) 1 μm.

mechanism regulating flagellar length is active even in fully grown flagella.

Several models have been proposed to explain the mechanism of ciliary/flagellar length regulation. Levy (1974) first proposed that length was regulated by the diffusion of a critical flagellar growth-limiting component into the flagellum. With the discovery of bidirectional intraflagellar transport (IFT) of large particles along flagellar microtubules to and from the distal tips (Kozminski et al., 1993; Orozco et al., 1999), where microtubule assembly and disassembly occurs, Marshall and Rosenbaum (2001) proposed that a flagellum reaches a defined length when IFT-dependent assembly is balanced with disassembly. Others have proposed that flagellar length may be determined by the quantity of tektin filaments associated with doublet microtubules (Norrander et al., 1995), or that Ca^{2+}-sensitive signal transduction systems regulate length or IFT motor switches (Tuxhorn et al., 1998).

Although each of these models explains certain behaviors of flagellar growth, the functional characterization of genes that regulate flagellar length will be necessary to build detailed molecular models for the regulatory mechanisms. Recent work from our laboratory has shown that *LF4* encodes a novel MAPK, indicating that a signal transduction pathway is necessary to enforce normal flagellar length (Berman et al., 2003). Here, we describe the characterization of the *LF3* gene and show that LF3p may associate with other *LF* gene products in the cell body. Two new insertional mutants in *LF3* have slow-growing, unequal-length flagella (Ulf) that accumulate IFT particles at their distal tips, suggesting an important role of LF3p in the coordinated assembly of the two flagella.

Results

A new phenotypic class of flagellar length mutants

WT *Chlamydomonas* cells have two flagella of equal length (Fig. 1 A), ranging from 10 to 15 μm. Using DNA insertional mutagenesis, we isolated a new class of mutants that have a striking Ulf phenotype. Here, we focus on two of these mutants, Ulf1 and Ulf3. When Ulf mutants were grown in dishes or tubes without aeration, many cells had pairs of flagella that were stumpy/short (Fig. 1 J). However, when Ulf cells were grown in liquid medium with vigorous aeration, most cells had flagella of unequal lengths (Fig. 1, E–I). The lengths of the shorter and longer flagella on individual cells are presented in Fig. 2 A. Many cells contained one short or stumpy (<1–2 μm) flagellum and a longer flagellum (Fig. 1, E and F), but pairs of flagella of a wide range of lengths were also present (Fig. 1, G and H). Some of the flagella reached lengths up to two times that of WT flagella (Fig. 1 I), similar to those previously seen in *lf* mutants. Because of the difference in the length of the two flagella, many cells spun slowly in liquid medium. In *Chlamydomonas* the two basal bodies differ in age and can be distinguished from each other based on their positions relative to the eyespot (Gaffal, 1988). In the uniflagellar mutant *uni1*, the single flagellum grows out from the basal body trans to the eyespot in >95% of uniflagellated cells (Huang et al., 1982). We examined the position of the longer flagellum in 69 Ulf cells but found no such positional bias.

Interestingly, when Ulf1 cells were grown under a 12-h light/12-h dark cycle with aeration, many cells had short flagella at the beginning of the light cycle and significantly longer flagella later in the day (Fig. 2 B). WT cells grown under similar conditions displayed fully grown flagella near the onset of the light cycle that did not elongate much over time (Fig. 2 B). The presence of short flagella on Ulf1 cells early in the light period and their gradual increase in length may reflect a slower rate of flagellar growth relative to WT cells. To test this, cells were deflagellated by pH shock and monitored for flagellar regeneration. Ulf1 cells regenerated their flagella much more slowly than WT cells

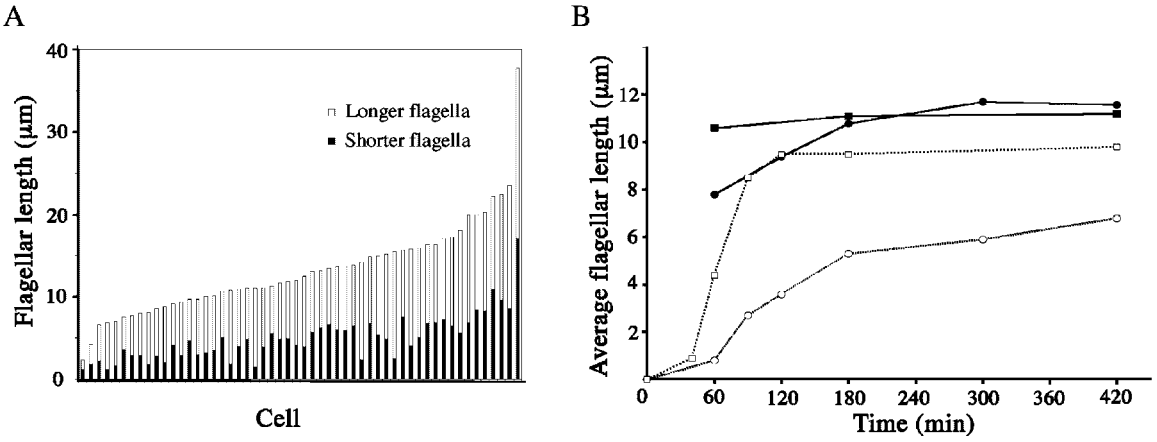

Figure 2. **Ulf1 cells grow flagella slowly and unequally.** (A) A histogram showing a wide variation of flagellar lengths in individual Ulf1 cells. The two flagella of a single cell often differ in length. (B) WT (squares) and Ulf1 (circles) cells were grown in M medium in bubblers for ~5 d, transferred to a 12-h light/dark cycle for 2 d and harvested by centrifugation. Half of the cells were resuspended in 4 ml of M medium in a 6-well microtiter plate (nondeflagellated cells, solid lines). The other half of the cells were deflagellated by pH shock (dotted lines), collected by centrifugation and resuspended in fresh M medium. Cells were incubated on a rotary shaker under constant light and samples taken at different times were fixed in glutaraldehyde for length measurement. Both flagella of a cell were measured for Ulf1 cells, but only one flagellum per cell was measured for WT cells because the two flagella were the same length. About 100 flagellated cells were used for measurement, except that 18 Ulf1 cells were measured at 60 min after deflagellation because only ~20% of cells had flagella.

(Fig. 2 B). These data suggest that flagellar assembly is considerably slower in Ulf1 cells than in WT cells.

Ulf1 and Ulf3 are alleles of the *LF3* locus

Because the Ulf mutants have cells with long flagella similar to previously identified *lf* mutants, we performed linkage analysis to determine whether they might be alleles of one of the known *LF* genes. Ulf1 was found to be closely linked to *lf3-2* on linkage group I (no recombinant in 17 random progeny). Ulf3 also mapped to linkage group I by its linkage to *ARG2* (in a cross with *arg2* mutants, nine parental ditype, one tetratype, and zero nonparental ditype). To determine if these two mutants belong to the same complementation group as *lf3-2*, we performed complementation tests in stable vegetative diploids. Diploids made between Ulf1 and WT cells all showed normal cell motility and >80% of these heterozygous diploid cells possessed flagella, all of which were <15 μm. Therefore, the mutation in Ulf1 is fully recessive to WT in diploids. It has been previously established that *lf3-2* is completely recessive to WT in diploids (Barsel et al., 1988). When stable diploids were constructed between Ulf1 and *lf3-2* mutants, >40% of cells in each Ulf1/*lf3-2* culture possessed long flagella that were 15–24 μm, a phenotype characteristic of the *lf3-2* parent. Similarly, the Ulf3 mutation failed to complement the *lf3-2* mutation in diploids. Together, these results indicate that Ulf1 and Ulf3 are mutant alleles of *LF3* and they are now designated as *lf3-5* and *lf3-6*, respectively.

The phenotypes of *lf3-5* and *lf3-6* mutants differ from that of *lf3-2* cells. When grown without aeration, most *lf3-5* and *lf3-6* cells had stumpy or short flagella. In contrast, <15% of cells had stumpy flagella and 30–80% of cells had abnormally long flagella in *lf3-2* (Fig. 1, K and L). Previous studies also indicated that all long-flagella *lf3* mutant alleles could regenerate their flagella after deflagellation, with kinetics similar to WT cells (Barsel et al., 1988).

LF3 null mutant flagella have normal axonemal structures but accumulate IFT-like particles at their distal tips

A striking feature of *lf3-5* and *lf3-6* is the presence of prominent swellings at the flagellar tips. The swellings were present on all nonregenerating flagella, regardless of lengths (Fig. 1, E–J, arrowheads), and on all flagella during regrowth after deflagellation. The size and morphology of the swollen tips of growing, nongrowing, and resorbing flagella were identical, as judged by high resolution differential interference contrast (DIC) microscopy (unpublished data). The bulbous flagellar tips (Fig. 1 N) of the mutants are distinctly different from the blunt or tapered tips of WT flagella (Fig. 1 M), although slight swellings were occasionally seen at the tips of regenerating flagella shorter than 2 μm in length (Fig. 1, B–D). Similar swellings were occasionally observed on the tips of *lf3-2* flagella (Fig. 1 L), although they were not found on all flagella and were less prominent than those on *lf3-5* and *lf3-6* cells.

When flagella and basal bodies of *lf3-5* and WT cells were examined using EM, we could find no differences between *lf3-5* and WT basal bodies, transition zones, or axonemal microtubules and associated arms, spokes, and central microtubules (Fig. 3 A, a). However, the distal tips of the flagella were filled with linear arrays of particles (Fig. 3 A, b–e) that resembled IFT particles found in WT flagella (Kozminski et al., 1993). To visualize the ends of flagellar microtubules, flagellated cells were attached to grids, extracted with nonionic detergent, and negatively stained. The A- and central microtubule capping structures appeared normal. The IFT material that filled the swollen flagellar tips appeared to be composed of strings of beaded structures (Fig. 3 A, f), similar to those described in first reports of IFT (Kozminski et al., 1993, 1995). These results indicate that *lf3-5* and *lf3-6* assemble normal axonemal structures but accumulate IFT particles at the distal ends of their flagella.

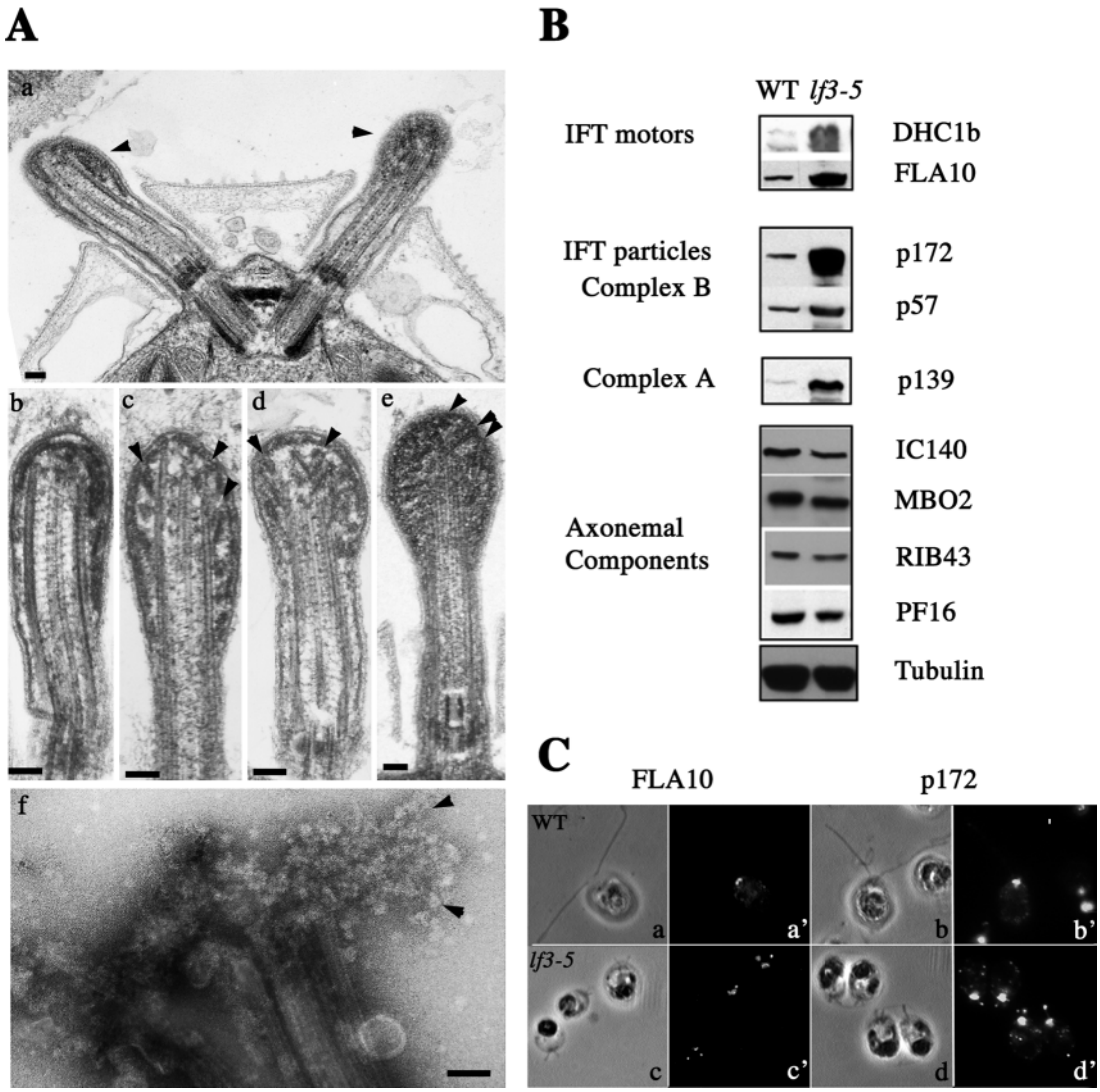

Figure 3. **Bulges at the tips of *lf3-5* flagella are filled with IFT particles.** (A) Thin-section electron micrographs of (a–e) flagellated cells reveal the tips of *lf3-5* flagella are filled with short linear aggregates of material (arrowheads) that resemble IFT particles. Negatively stained (f) NP-40 extracted flagella show linear arrays of particles hanging at the tip. Bars, 100 nm. (B) Immunoblots reveal the accumulation of IFT motors and particle complex A and B proteins in *lf3-5* flagella. Equal amounts (30 μg) of purified flagella from WT and *lf3-5* cells were reacted successively with antibodies against IFT motors (FLA10, DHC1b), IFT complex components (p172, p57, p139) and axonemal structural proteins (IC140, MBO2, RIB43, PF16, Tubulin). (C) DIC (a, b, c, and d) and immunofluorescence (a′, b′, c′, and d′) images of WT and *lf3-5* cells. In WT cells (a and b), the peribasal body region was brightly stained by anti-FLA10 and anti-p172. Faint staining of WT flagella was observed but was not visible under the exposures used. Antibodies against FLA10 and p172 reveal a concentration of staining at the flagellar tip bulges and around the basal bodies in (c and d) *lf3-5* cells.

lf3-5 flagella accumulate an unusual amount of IFT proteins at their tips

To confirm that the swollen tips contained IFT particles, isolated *lf3-5* and WT flagella were compared by immunoblots using antibodies to IFT components. Immunoblot analysis of isolated flagella (Fig. 3 B) revealed that *lf3-5* flagella accumulated a greater amount of FLA10 (an anterograde kinesin II motor protein; Walther et al., 1994; Kozminski et al., 1995), p139 (an IFT complex A protein, Cole et al., 1998), p57 and p172 (IFT complex B proteins; Cole et al., 1998), and DHC1b (a cytoplasmic heavy chain dynein; Pazour et al., 1999; Porter et al., 1999) than did WT flagella. By contrast, relative to WT, *lf3-5* flagella contained similar or slightly decreased levels of the axonemal structural proteins, PF16, IC140, RIB43, and MBO2. To confirm that the IFT components are accumulated at the distal tips, flagella were examined by immunofluorescence microscopy. Antibodies to FLA10 and p172 strongly stained the peribasal body region and the swollen tips of *lf3-5* cells (Fig. 3 C, c and d). An antibody to p139 produced similar results (unpublished data). These antibodies stained the peribasal body complex and showed weak staining along the axoneme and at the tips of WT cells (Fig. 3 C, a and b). Together, these results demonstrate that flagella of *lf3-5* accumulate excessive amounts of IFT proteins at the distal swellings of their flagella.

Cloning of the *LF3* gene

The insertion of the nitrate reductase gene in *lf3-5* allowed us to clone the WT *LF3* gene. We showed that a λ bacteriophage clone λ12D9 (Fig. 4 A) could restore WT motility

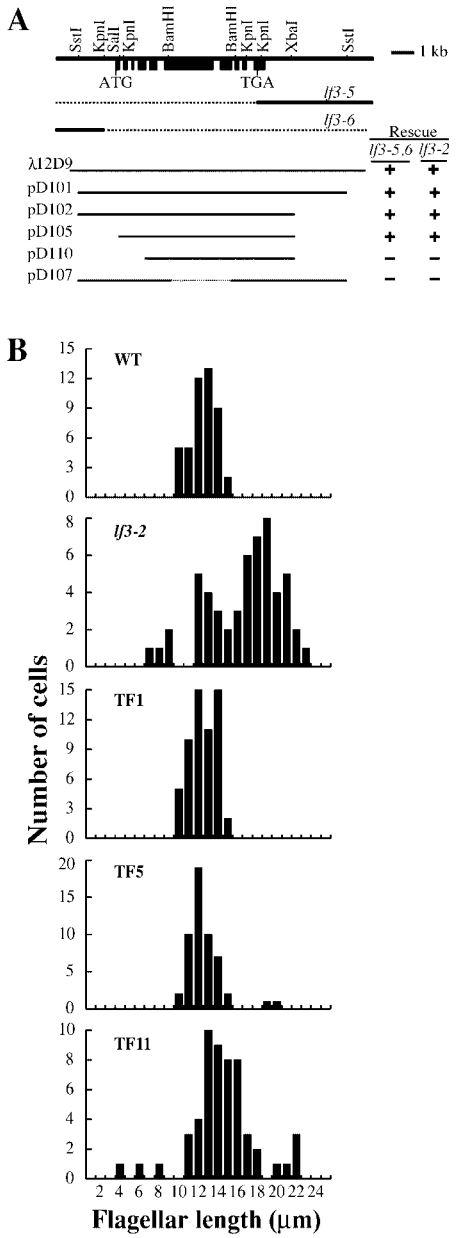

Figure 4. **Phenotypic rescue of *lf3-2*, *lf3-5*, and *lf3-6* mutants with cloned DNA fragments.** (A) A restriction map of the *LF3* gene region. Exons are represented with black boxes and putative start and stop codons are indicated. *lf3-5* and *lf3-6* mutants have extensive deletions of the genome (dotted lines) covering the *LF3* locus. Six genomic clones were cotransformed with the pARG7.8 plasmid into the deletion mutant strains or the long-flagella mutant *lf3-2* containing the *arg2* or *arg7* mutations to test for the rescue of the flagellar length phenotype. Only genomic clones containing all the putative exons could restore the WT phenotype to the mutants. pD107 with an internal deletion of a 3-kb BamHI fragment, did not rescue the mutant phenotype. (B) Flagellar length distributions in WT cells, the *lf3-2* mutant cells, and three strains (TF1, TF5, and TF11) in which the *lf3-5* mutant phenotype was rescued by transformation using an HA-tagged *LF3* gene are shown. Aflagellate cells (<10% of the total) are not included in the histograms.

to *lf3-5* cells upon introduction into cells by cotransformation with the pARG7.8 plasmid. Using restriction fragments from this genomic region as hybridization probes on DNA blots, we determined that both *lf3-5* and *lf3-6* mutants contained extensive deletions around the *LF3* locus (Fig. 4 A). Subclones of this genomic region were transformed into cells with the *lf3-2*, *lf3-5*, or *lf3-6* mutations to delineate the extent of the *LF3* gene. Plasmid pD105 contains the smallest fragment that could rescue all three mutants upon transformation (Fig. 4 A).

```
   1  MPLRLGDFDG EAQERQTDDG IAAFCRHLGE LCDLLNAPYD DVNALAHLAR
  51  AGELQGTNVN LLLHNAFYHW LGERVQLSVA ESRDVAPETI AAHAREAALA
 101  QIQSGEYVSQ FVTAVAAHAT QNVDGVQGPV APTKQSLFDL PGHFELLGPD
 151  EVDGLLKDLA SSDCPVGALE KLVADPHLLE DLCFGPTWPQ LCDSLGRLVC
 201  LLPPSGGTQA AVTGAGHHQH GHTRAAAAVG GGAGRAAASV PEMPKQHELL
 251  LQALNEVVSA VAASSPPHAA ELLDGLAPYL TALALRLSLP LPGAGTGHAT
 301  PVAPDQLQTR VQAGMAGPGA GAGDGGPGGV AVVGTGAVGL LVAVTARDAF
 351  AVEIVRLAQQ LVVGLSQEFH TLPHSCAALA ARAVCDVVRA GLARGAPAPP
 401  PPAGAVTAAS GGGGPGGGGL ADLDLELSAL DLLVLLDPEL RWWQRLCSST
 451  HATQRMADAA AATQLAAALE AALAAWAYAT AAAAAAAGHH SDGGLAVAVA
 501  AAGVRSPSHL VACAALLGGL VRANNPALLA CEQPAGSRRV VGALPAVVAA
 551  PAPAPAPHVA NGHSGVGTGG LSSAGVEGLP VAMAAALPQG AGAAAAGATG
 601  PASGAQAAAA LPEYSEVPQY TPAQVAEQRQ RETRLLGALC GVACALADRP
 651  GLERPGGAGH DSGTGGARGS VFVTLAADVL AAAAELGVLT WHQPMAPGAH
 701  GGTSAAVAGA AGGNGGAGGG ALAALLQAMM RAASVTAAAA AAAGAAGNGG
 751  AGTGGRTRAA AAAEADAWLE AATCVLEAVA EHAELGAASS PTALPPPALS
 801  VSDALSGLLR HIAGRVRGCA GGGGGGGAAG TNSAAASAAA ATAAPAWSRA
 851  VVPLAVAAAP QSPLVAAALT DLAEPLCALL TARSARRTAS AAKAAAAATA
 901  AQAAGKAAAV AAAPAAAAPA LAASGSSGDA AAGLAASLSL LDILSGGSSS
 951  KSVTAACPGT AATAAGRGEV GTAPPPPPPP PLQAVELDAM EELAAALVLS
1001  YCRGGAAAIA EPVAAVQPSG VLSNAGDGGG SSGTIAGLTA GAGAGACAAP
1051  CAPQPVAALP QQLQRPALLT CAARSLCRRY DTAGLVYAVP PSGSVEEELR
1101  EGGAGSEAEE PEVPAAEAHP GGGLLSIRGG SGVACAATAA QRRAVAAAGG
1151  LARSCPAGQQ ALLAEGFARR LLRDVAATLH EGEYTSPLCE PLAYADPLAG
1201  LAAALAELMA WPGLLAVLQP VQAQPDAVAA AAGAGAPAAA GAGVGAGSGA
1251  RQRLAQETAD RARAEVLVLL QELVTWLDPC CDDSRGVAPQ DAAAVSLAAF
1301  RSLVEHDPGA AAALDADTNI RWYLCNLTGD DAPPAAPPAE CVAPQSDMLL
1351  DLARRLLAAL PPLAAAAAPG AAPA
```

Figure 5. **Predicted protein sequence of *LF3*.** The leucine residues of a putative leucine zipper motif (http://us.expasy.org/prosite/) are highlighted in black. Putative transmembrane helices are underlined. A PEST sequence predicted by the program PEST-find (http://www.at.embnet.org/embnet/tools/bio/PESTfind/) is shaded. The arrowhead indicates the position at which three copies of the HA epitope were inserted. The glutamine codon at position 209 mutated to an amber stop codon in *lf3-2* is boxed and the next downstream methionine is indicated in bold. Sequence data are available from GenBank/EMBL/DDBJ accession no. AY186602.

Flagellar lengths of independent strains obtained by rescuing *lf3-5* or *lf3-6* mutants with the cloned *LF3* gene showed significant variations and fall into three phenotypic groups: (1) entire populations of cells had flagella of normal length and morphology (e.g., Fig. 4 B, TF1); (2) >90% of cells had normal-length flagella but 1–10% of cells consistently had abnormally long flagella (e.g., Fig. 4 B, TF5); and (3) most of the cells in a population had abnormally long flagella (e.g., Fig. 4 B, TF11). The phenotypic variations among rescued strains may be caused by different levels of expression or by different modifications of the cloned *LF3* gene that integrated into the genome of the transformants.

A 7.5-kb region of genomic DNA containing the area of overlap between the deletions in the two *lf3* mutants and the fragment cloned in pD105 was sequenced and analyzed by the GeneMark and Genscan programs to identify putative coding regions. Primers were designed to perform reverse

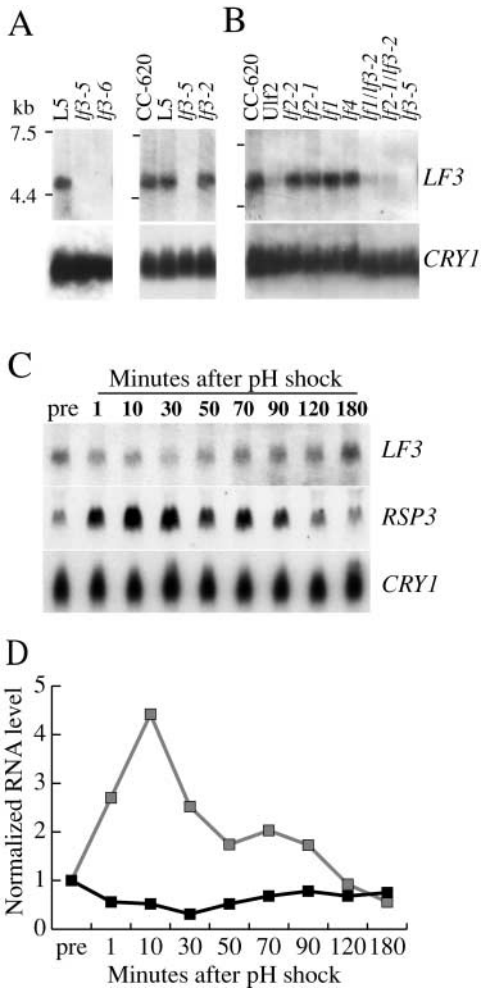

Figure 6. **RNA-blot analysis of the *LF3* transcript.** (A and B) 25 μg of total RNA from a number of mutant and WT (L5, CC-620) strains was loaded in each lane and the *LF3* transcript was detected with a hybridization probe corresponding to the 5′ region of the gene. (C) Accumulation of the *LF3* and *RSP3* transcripts before (pre) and at different times after deflagellation of WT cells (strain 3D). The level of the transcripts was quantified and shown in (D) y-axis values: radioactivity of the *LF3* transcript (closed squares) and the *RSP3* transcript (open squares) normalized to the level of the *CRY1* transcript used as loading control. The predeflagellation value is set as one.

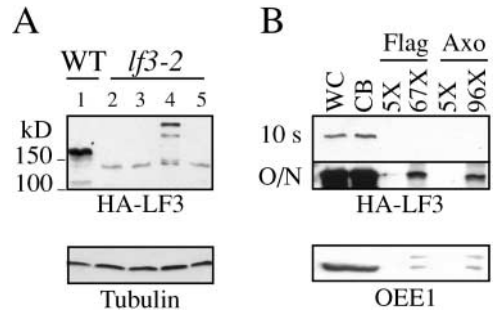

Figure 7. **HA-LF3p is localized to cell bodies and a truncated protein is made from the *lf3-2* allele.** (A) Western blots of total cell proteins (10^6 cells) from transformed strains rescued with either a WT construct or a mutant *lf3-2* construct tagged with the HA epitope, detected with an anti-HA mAb. The transformant in lane 4 shows some bands of higher molecular masses, but none are the same size as the WT protein. The blot was labeled with a mAb to β-tubulin to show loading. (B) Whole-cell (WC) and cell-body (CB) proteins from 10^6 cells, purified flagella (Flag), and axonemes (Axo) from 5, 67, or 96× the amount of cells in the CB lane were analyzed on immunoblots. Two images of the same blot are shown, obtained after a 10-s or overnight (O/N) exposure. The presence of a trace amount of cell-body contamination in the flagellar and axonemal preparations was revealed using an antibody to OEE1.

transcriptase PCR (RT-PCR) from RNA to obtain a 4.7-kb cDNA sequence. Comparison of the genomic and cDNA sequences indicates that the transcribed region consists of 10 exons separated by nine introns. The cDNA sequence contains a long open reading frame that predicts a 133-kD polypeptide of 1,374 residues (Fig. 5). Extensive searches of protein, EST and genomic sequence databases, as well as protein structure databases, uncovered no homologous polypeptides. The predicted polypeptide contains an unusually high content of alanine (25.7%), glycine (12%), and leucine (11.9%). Potential functional motifs identified in the sequence include a putative leucine zipper motif between residues 632 and 653 that may mediate protein–protein interaction (Prosite entry: PDOC00029), several potential transmembrane helices (Fig. 5, underlined), and a PEST sequence (with a significance score of 7.65 predicted by PEST-find; Fig. 5, shaded). PEST sequences in other proteins are involved in targeting proteins for degradation by proteasomes (Rechsteiner and Rogers, 1996).

RNA analysis

To identify the *LF3* RNA transcript, total RNA from WT cells, *lf3-2*, *lf3-5*, and *lf3-6* mutants was analyzed on RNA blots with hybridization probes corresponding to the 5′ region of the gene (Fig. 6 A). A 4.8-kb transcript that closely matched the size of the deduced cDNA sequence was detected in WT RNA. *lf3-5* and *lf3-6* cells did not produce the corresponding transcript, which is consistent with our hypothesis that they contain null mutations of *LF3*. Unlike the null mutants, *lf3-2* expressed an *LF3* transcript of similar size and abundance as the transcript in WT cells.

Previous studies of *lf1*, *lf2*, and *lf3* mutants have shown that their gene products may interact (Barsel et al., 1988). In double *lf* mutant strains, many cells had stumpy flagella and Ulf, similar to *lf3-5* and *lf3-6*. We analyzed total RNA from a number of strains to determine whether the level of the *LF3* transcript was affected by mutations in other *LF* loci (Fig. 6 B). No significant decrease in the level of the *LF3* transcript was detected in *lf1*, *lf2*, or *lf4* mutants, but a decrease was observed in a third Ulf insertional mutant (Ulf2) that contains a null mutation at *LF2* (unpublished data). Strikingly, *LF3* transcripts were dramatically reduced in double mutant strains of *lf1 lf3-2* and *lf2-1 lf3-2*, suggesting that the synthetic Ulf-like phenotype of double *lf* mutants may be caused by reduced *LF3* expression.

Levels of RNA transcripts for many flagellar components, such as the radial spoke protein RSP3 (Fig. 6, C and D), increase dramatically when flagella are amputated. We examined the level of the *LF3* transcript in WT cells at various times after deflagellation. Rather than increasing, the level of the *LF3* transcript appeared to decrease slightly in the first 30 min (Fig. 6, C and D), suggesting that LF3p may not be a component of the flagella.

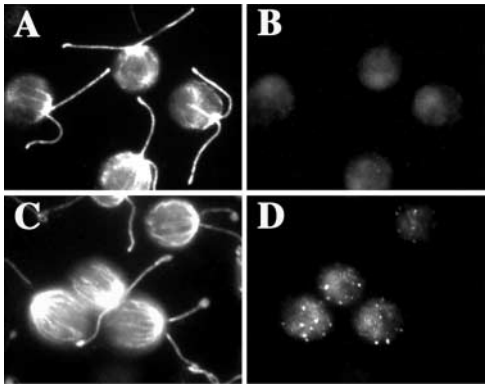

Figure 8. **Immunofluorescence localization of the HA-tagged LF3 protein to punctate spots in the cell body.** (A and B) Control cells without the HA-tagged gene. (C and D) Rescued *lf3-5* strains expressing the HA-tagged *LF3* gene. Cells were doubly stained with antibodies to α-tubulin (A and C, Texas red) and the HA-epitope (B and D, FITC).

Epitope tagging of the LF3 protein

Attempts to prepare antibodies to LF3p or constituent peptides were unsuccessful. As an alternative approach, we tagged the *LF3* gene with the HA epitope (Fig. 5). The tagged gene rescued the *LF3* null mutants upon transformation as well as the untagged construct did. A mAb against HA detected with high specificity an ~160-kD polypeptide in cells that received the tagged gene (Fig. 7 A, lane 1; and Fig. 9 A). When proteins from cell bodies, flagella, and axonemes were analyzed on immunoblots, most of the tagged protein was found in the cell body (Fig. 7 B). A small amount of the tagged protein was detected in flagella and axonemes, but a similar amount of the chloroplast protein OEE1 was present in the same samples, suggesting that these preparations were contaminated by a small quantity of proteins from cell bodies.

Cells expressing HA-LF3p were examined by immunofluorescence microscopy using the HA antibody. The tagged protein was found in discrete spots throughout the cell that did not appear to associate with any particular organelles, and no staining was observed in the flagella (Fig. 8). We examined two different HA-tagged strains that expressed different levels of the protein to test the possibility that the punctate pattern of staining was an artifact caused by overexpression of the protein from the transgene. Despite brighter staining seen on cells expressing a higher level of the HA-tagged protein, the overall localization of LF3p was similar in both cell lines (unpublished data), indicating that the punctate staining in the cell was probably not a consequence of protein overexpression. We conclude that most, if not all, of the tagged LF3p is localized to the cell body and not the flagella.

The *lf3-2* allele contains an amber mutation

To characterize the genetic lesion in *lf3-2*, we amplified and sequenced the mutant gene by both genomic PCR and RT-PCR. A single transition mutation that changes the codon CAG (glutamine; Fig. 5, boxed) to an amber stop codon UAG was detected at position 209. Termination of translation at the amber codon would produce only a short protein of 208 aa from the NH_2-terminal region. A polypeptide of this length should not be functional based on earlier works using truncated plasmid constructs to attempt phenotypic rescue upon transformation. One subclone that has an internal deletion of the coding region, pD107, would be predicted to produce a protein product of at least the first 436 residues, but it did not rescue the *lf3* mutants upon transformation (Fig. 4 A).

One possible explanation for the observation that the *lf3-2* amber mutation does not produce the null phenotype is that a truncated protein is produced by reinitiation of translation at an AUG (Fig. 5, the corresponding methionine is in bold) 34 residues downstream of the amber mutation in this mutant. To test this possibility, we created an HA-tagged *lf3-2* construct and transformed it into the *LF3* null mutants to create strains expressing the tagged mutant protein. Strains

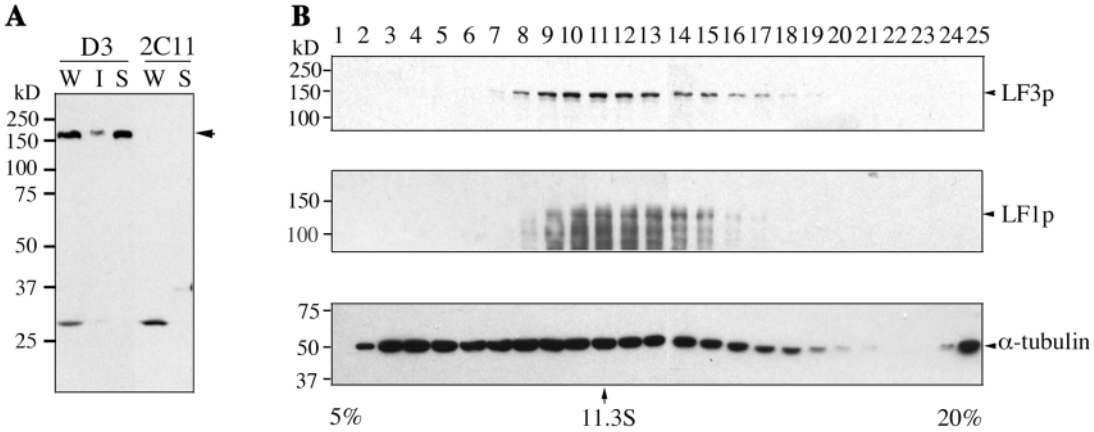

Figure 9. **LF3p and LF1p cosediment in sucrose density gradients.** (A) Cells expressing an HA-tagged *LF3* construct (D3) and control cells without the HA-tagged gene (2C11) were extracted by repeated cycles of freezing/thawing. Whole cells before extraction (W), and insoluble (I) and soluble fractions (S) from equal number of cells after extraction were analyzed by SDS-PAGE and immunoblotting with the anti-HA antibody. (B) Cell extracts of two strains expressing HA-LF3p and HA-LF1p were analyzed in parallel on a 5–20% sucrose density gradients. Fractions were collected from top (5%) to bottom (20%) of the gradients and analyzed on 8% SDS-PAGE. HA-LF1p was highly labile during extraction but both the intact polypeptide (120 kD) and degraded products comigrated with HA-LF3p. Sedimentation of α-tubulin in the same gradient fractions is shown for reference.

that received the mutant construct all produced a protein of ~130 kD (Fig. 7 A), 30 kD smaller than the full-length LF3p, which is consistent with our prediction of the size of a protein made by translational reinitiation. Moreover, the truncated protein was expressed at a lower level than the full-length product (Fig. 7 A). Based on these observations, we propose that the *lf3-2* allele is a hypomorphic allele producing either a partially functional protein or too little of the truncated protein.

LF3p is part of a ~11S complex in the cytoplasm

Most of the HA-LF3p could be released from whole cells by repeated cycles of freezing in liquid nitrogen and thawing or by treating cells with 0.2% NP-40 (Fig. 9 A). To determine if LF3p exists as larger complexes in the cytoplasm, we fractionated extracts prepared by each method on 5–20% sucrose density gradients (Fig. 9 B). HA-LF3p sedimented at ~11S, regardless of the methods used for preparation of the cell extracts. The *LF1* gene has recently been cloned and the protein was similarly tagged with HA (unpublished data). Parallel analysis of cell extracts containing the HA-LF1p showed that it sedimented with the HA-LF3p on sucrose density gradients (Fig. 9 B). This finding provides the first biochemical evidence that LF1p and LF3p may be part of a common cytoplasmic complex that regulates flagellar length.

Discussion

Ulf1 and Ulf3 mutants are alleles of the *LF3* locus

More than 20 mutants with abnormally long flagella have been shown to identify four unlinked genetic loci, *LF1*, *LF2*, *LF3*, and *LF4* (McVittie, 1972; Barsel et al., 1988; Asleson and Lefebvre, 1998). Here, we characterized two Ulf mutants and showed that both mutations are null alleles (*lf3-5* and *lf3-6*) of the previously identified *LF3* gene. An 8-kb genomic DNA clone that contains a single predicted transcript restored normal-length flagella to mutant cells upon transformation into *lf3-2, lf3-5*, and *lf3-6*. The entire coding region of *LF3* was deleted in *lf3-5* and *lf3-6*. The long-flagella *lf3-2* allele contained an amber mutation within the predicted coding region. By epitope tagging, the *lf3-2* mutant gene was found to produce a truncated protein in reduced quantity. Together, these data indicate that the Ulf phenotype is due to null mutations and the long-flagella phenotype is caused by hypomorphic mutations of the *LF3* gene.

LF3p plays a role both in flagellar assembly and length control

Although flagella are shorter in the null mutants than in *lf3-2*, it is not clear that there is a difference in the preset value of flagellar length in these two classes of *lf3* mutants. In synchronous populations of *lf3-5* cells, flagella were short but gradually grew to abnormally long lengths during the light period. Similarly, during flagellar regeneration after deflagellation, *lf3-5* flagella grew slowly and unequally. By contrast, the length of flagella on WT cells showed no significant changes during the day, and both flagella on WT cells grew at the same rate and reached full length within 2 h after deflagellation. It is possible that *lf3-5* differs from *lf3-2* by assembling flagella much more slowly, therefore taking longer to assemble long flagella. The slow flagellar growth defect of *lf3-5* indicates that the *LF3* gene product plays a role in flagellar assembly as well as in regulating the length of the two flagella. The defective protein product produced by the mutant *lf3-2* gene allows flagellar assembly with rapid kinetics seen in WT cells, but does not prevent flagella from growing to excess length. The phenotypic defect in *lf3-2* may be due to the lack of the NH_2-terminal portion of the protein, and/or to the reduced level of the truncated product.

The tips of flagella in *LF3* null mutants are filled with IFT particles

A striking feature of the *LF3* null mutants is the presence of bulges at the distal ends of their flagella. Immunofluorescence microscopy showed that IFT proteins accumulated in the bulged tips and EM revealed linear strings of IFT-like particles that filled the bulged tips. Although a handful of short or stumpy flagella mutants show distal tip swellings on their flagella (Huang et al., 1977; Jarvik and Chojnacki, 1985; Pazour et al., 1999; Porter et al., 1999), the presence of distal bulges was not restricted to short flagella in the *LF3* null mutants. The bulges were present on flagella of all lengths and at all stages of growth in these *lf3* mutant cells. Although some IFT particles appear to accumulate at the tips of regenerating WT flagella (Deane et al., 2001), we did not detect bulged tips or collections of particles in both nonregenerating and regenerating flagella of WT cells. On the other hand, the enlarged flagellar tips are found in mutants with abnormally long flagella, including *lf3-2* (this paper), *lf1*, and *lf2* (McVittie, 1972; unpublished data). Accumulations of IFT proteins at the flagellar tips have also been shown by immunofluorescence microscopy in *lf1-1* and *lf3-2* mutants (Perrone et al., 2003). Therefore, distal bulges filled with IFT particles appear to be a defect associated with a number of *lf* mutants, and these bulges are especially pronounced when the *LF3* gene product is absent.

LF3p may play a role in regulating IFT

There is abundant evidence that IFT and the motors responsible for IFT are important for flagellar growth and maintenance (for reviews see Rosenbaum and Witman, 2002; Cole, 2003). Mutants with defects in either the anterograde motor protein or components of IFT complex B fail to assemble flagella or assemble very short flagella. In these mutants, IFT particles do not accumulate in the flagella (Pazour et al., 2000; Brazelton et al., 2001; Matsuura et al., 2002). Mutants defective in the retrograde motor or deficient in proteins of IFT complex A have stumpy or short flagella that accumulate IFT particles at the tips or along the length of their flagella, similar to *lf3-5* (Pazour et al., 1998, 1999; Piperno et al., 1998; Porter et al., 1999; Iomini et al., 2001). Interestingly, cells with mutations in the dynein light chain LC8, a component of the retrograde motor, also have Ulf (Pazour et al., 1998). The *lf* mutants differ from known IFT mutants in that they grow abnormally long flagella and the accumulation of IFT particles appears to be restricted to the tips. The role of LF3p in the accumulation of IFT particles at the flagellar tips is intriguing. LF3p is a novel protein with no

homology to known IFT components and it does not colocalize with IFT proteins in the flagella or near the basal bodies. Because most of the IFT proteins are present in the cell body and there is a constant bidirectional reshuffling of IFT particles between the cell body and flagella, LF3p might interact with IFT components in the cytoplasmic compartment to regulate their transport in the flagella. Iomini et al. (2001) determined that IFT particles moving from the base to the tip of a flagellum or from the tip to the base differ in size, velocity, and frequency, indicating that the IFT particles and their motors must undergo some forms of modification at both the proximal and distal ends of the flagellum. One possibility is that LF3p alters the ability of IFT complexes to release flagellar cargoes at the tip or alters the ability to pick up flagellar material that needs to be returned to the cell body. Alternatively, LF3p activity may affect the switches that regulate the activity of the anterograde motor and the retrograde motor at the base and tip of the flagella. An inhibition in the release of flagellar components or in the activation of motor switches in *lf* mutants could explain the accumulation of IFT particles at the ends of the flagella.

A simple model that assumes the steady-state length of the flagella is maintained by a balance of flagellar assembly and disassembly has recently been proposed (Marshall and Rosenbaum, 2001). Longer flagella could result either from an increased assembly rate or a decreased disassembly rate. Using HA-tagged tubulin as a marker, the turnover of tubulin at the tip of a long-flagella mutant, *lf2-5*, was shown to be reduced relative to WT cells, suggesting that in this mutant the longer flagella may be due to decreased disassembly. One obvious defect we detected in *lf3-5* cells is that their flagella grow slowly, indicating a defect in flagellar assembly. Because the overall assembly rate is already reduced, if flagellar length is determined simply by a balance of assembly and disassembly, one would predict that the disassembly rate must be dramatically reduced to give rise to the striking flagellar phenotype of *lf3-5*. This prediction can be tested by measuring the turnover rate of tubulin at the flagellar tip of this mutant.

The association of a length-control defect and an assembly defect in the *LF3* null mutants with the accumulation of IFT particles at the growing tips of their flagella is consistent with the possibility that flagellar length is regulated at least in part by regulating IFT. However, there is no indication of how IFT is regulated. The primary protein sequence of LF3p gives no obvious clues about its mechanism of action. The hydrophobic nature of the protein and the presence of putative transmembrane domains suggest that LF3p may be membrane associated. Consistent with this, a small amount of the LF3p was retained in the crude microsomal membrane fraction obtained by differential centrifugation in the fractionation works (unpublished data). However, the observation that LF3p can be extracted from cells by freezing and thawing indicates that most of the protein is soluble in the cytosol or only loosely associated with membrane structures. The protein has extensive glycine-rich regions that may be important for protein–protein interaction, and such regions are also found in the gene product of *LF1* (unpublished data) and *LF4* (Berman et al., 2003). The presence of a PEST sequence in LF3p suggests that the protein may be targeted for degradation in proteasomes after ubiquitination, raising the interesting possibility that the level of LF3p and its interacting proteins may be regulated by proteolysis.

Interaction of LF3p with other *LF* gene products

Several lines of evidence suggest that *LF1*, *LF2*, and *LF3* may function in the same regulatory pathway(s). First, double mutants of any pair of mutant alleles at these three loci produce cells that are flagella-less or uniflagellated (Barsel et al., 1988). In the present work, we reexamined two double mutants (*lf1 lf3-2* and *lf2-1 lf3-2*) and noticed that their phenotypes are in fact similar to the null mutants of *LF3*. Second, previous works have shown that whereas mutants in different *LF* genes can complement each other in stable diploids, the long-flagella defect cannot be fully corrected in temporary quadriflagellated dikaryons formed between gametes of two different *lf* mutants (Barsel et al., 1988). This result suggests that some key factor(s) may be absent from the cytoplasm of *lf1*, *lf2*, and *lf3* mutants, and that these factors cannot be synthesized or assembled rapidly enough to function in temporary dikaryons. In the present work, cosedimentation of LF3p with another LF protein, LF1p, in sucrose density gradients provides the first biochemical evidence to support the possibility that these proteins may interact with each other and form a complex in the cytoplasm. In addition, both LF1p and LF3p are localized to similar punctate spots in the cell (unpublished data). We have recently cloned the *LF2* gene and our preliminary analysis shows it shares similar localization and sedimentation properties with LF3p and LF1p. These findings strengthen the working model that LF3p forms a cytoplasmic complex with at least two other LF proteins, LF1p and LF2p, in regulating flagellar length and flagellar assembly. LF1p is another novel protein with unknown functions, but *LF2* encodes a serine/threonine kinase (unpublished data). Genetic studies indicated that the fourth *LF* gene, *LF4*, may function downstream of the first three *LF* genes (Asleson and Lefebvre, 1998) and it encodes a MAPK (Berman et al., 2003). The identification of the gene products of *LF3* and the other *LF* genes opens up exciting opportunities to uncover the molecular mechanisms that regulate flagellar assembly and flagellar length.

Materials and methods

Strains and culture conditions

Chlamydomonas strains CC-620 (*Chlamydomonas* Genetics Center), our laboratory strains 3D, 1A (derivatives of 137c), and L5 (*nit1, apm1-19, mt*$^+$) were used as WT strains. Two insertional mutants, Ulf1(12D9) and Ulf3 (29H4), with an Ulf phenotype, were obtained by DNA insertional mutagenesis using pMN24, a plasmid containing the nitrate reductase structural gene (Tam and Lefebvre, 1993). A long-flagella mutant, *lf3-2*, was described previously (Barsel et al., 1988). Cultures were routinely maintained in liquid M or TAP medium (Harris, 1989) in 24-well microtiter plates under continuous illumination, unless otherwise specified.

Light and electron microscopy

Cell motility was examined under a dissecting microscope (Carl Zeiss MicroImaging, Inc.) at a magnification of 80 and flagella of cells fixed in 0.5–1.25% glutaraldehyde were examined under phase contrast microscopy (model Axioplat; Carl Zeiss MicroImaging, Inc.). For flagellar length measurement, DIC images of 50–100 cells were captured using a Diaplan (100× Leitz objective, NA 1.25; Leica) or a microscope (63 or 100× objective, NA 1.4; model Axioplan 2IE; Carl Zeiss MicroImaging, Inc.) and a video camera (model CCD-72; DAGE-MTI, Inc.; or an Orca ER camera;

Hamamatsu). Flagella on captured images were analyzed with Scion Image 1.59 software (NIH) or Openlab software (Improvision Inc.).

Thin-section EM of whole cells was performed as described previously using a JEOL microscope (model 1200EXII; Porter et al., 1999). For negative staining, drops of concentrated cells in culture medium were placed on carbon/formvar-coated copper electron microscope grids. Cells were allowed to settle for 30–90 s, medium was drawn off the grid with a pipette, grids were inverted over two to three drops of 1% aqueous uranyl acetate and air dried. For detergent extraction, flagellated cells were attached to carbon/formvar grids coated with 0.2% poly-L-lysine and excess medium was drawn off with a pipette. Grids were inverted over drops containing 50 mM Hepes, pH 7.2, 3 mM $MgSO_4$, 1 mM EGTA, and 0.001–0.01% NP-40 for 30 s. Grids were inverted over several drops of buffer without NP-40, and stained with 1% uranyl acetate. Images were captured on film and scanned into digital format, or with a video capture system (model Mega View II; Soft Imaging System). All DIC and EM images were assembled using Adobe Photoshop 7.0.

Genetic analysis

Dominance/recessiveness tests of the Ulf1 mutant and complementation tests between Ulf1, Ulf3, and *lf3-2* were performed by mating strains with complementing auxotrophic markers, *arg7* and *nit1*, and selecting stable diploids on minimal nitrate medium. Multiple (16–24) diploid strains were recovered and examined in each cross.

Cloning and sequencing of the *LF3* gene and the mutant *lf3-2* allele

A previous work indicated that the mutation in *lf3-5* was caused by the integration of two copies of pMN24 (Tam and Lefebvre, 1993). A 7.5-kb region flanking the integrated plasmid in *lf3-5* was cloned by digesting the mutant DNA with SalI and performing plasmid rescue as described previously (Tam and Lefebvre, 1993). A 4-kb PstI–SstI fragment from the cloned region was used as a hybridization probe to screen a λ phage library of *Chlamydomonas* WT genomic DNA and positive clones were tested for phenotypic rescue of *lf3-5* or *lf3-6* mutants by cotransformation using the pARG7.8 plasmid (Debuchy et al., 1989) as described previously (Tam and Lefebvre, 1993). Fragments of a lambda clone λ12D9, which was able to rescue the mutant phenotype, were subcloned into the vector pBluescript KS+ (Stratagene) using restriction sites indicated in Fig. 4 A. These subclones were tested for phenotypic rescue of *lf3-2*, *lf3-5*, and *lf3-6* by cotransformation. Nested-deletion clones for sequencing were made using Exonuclease III (New England Biolabs, Inc.) and S1 nuclease (GIBCO BRL) according to Sambrook et al. (1989). The sequence of the *LF3* gene was obtained by sequencing plasmid clones with universal sequencing primers or gene-specific primers (DNA Sequencing and Synthesis Facility, Iowa State University, or Advanced Genetics Analysis Center, University of Minnesota). The gene prediction programs GeneMark (http://opal.biology.gatech.edu/GeneMark/eukhmm.cgi) or Genscan (http://genes.mit.edu/GENSCAN.html) were used to predict the exon/intron structure of *LF3*.

cDNA sequences were obtained by RT-PCR using primers designed for putative exons under conditions described previously (Tam and Lefebvre, 2002), except that RNA was treated with amplification-grade DNaseI (GIBCO BRL) for 15 min at RT to remove DNA contamination before reverse transcription. PCR products were sequenced after purification using the Microcon PCR purification kit (Millipore) or after cloning into PCRII (Invitrogen). 5′ RACE was performed with gene-specific primers in the second exon according to the protocol of Finst et al. (2000). 3′ RACE was performed using the 3′ RACE kit from GIBCO BRL.

To determine the genetic lesion in the *lf3-2* allele, we sequenced overlapping genomic PCR products covering the entire coding region, as well as RT-PCR products from the *lf3-2* mutant with a series of gene-specific primers. The mutation in *lf3-2* was verified by sequencing additional PCR products of the region of interest derived from multiple WT strains and *lf3-2* subclones.

RNA analysis

Total RNA was isolated by LiCl precipitation as described by Wilkerson et al. (1994), except that 100 μg/ml of proteinase K was used in the lysis buffer. Cells were deflagellated by pH shock and allowed to regenerate their flagella under light. Samples were taken at different times for RNA isolation. Total (25 μg) RNA was size-fractionated in 1% MOPS-formaldehyde agarose gels following the protocol of Sambrook et al. (1989) and transferred to Brightstar Plus membrane (Ambion). A 2-kb SalI–BamHI fragment or an RT-PCR product of the same region was labeled with [^{32}P]dCTP for use as a hybridization probe. Membranes were hybridized in ULTRAhyb™ (Ambion) with labeled probes at 42–44°C overnight, washed sequentially in 2× SSC and 0.2× SSC solution containing 5 mM EDTA and 0.2% SDS at 65–68°C. Radioactivity on membranes was measured by exposing them to a phosphor screen, which was subsequently quantified with a STORM 840 imager and analyzed with ImageQuant v1.2 (Molecular Dynamics). Membranes were rehybridized without stripping using labeled DNA from the *CRY1* gene (encodes the S14 ribosomal protein) to monitor loading.

Epitope tagging, immunoblot, and immunofluorescence analysis

Three copies of the HA epitope obtained from plasmid p3XHA (Silflow et al., 2001) were inserted into one of the SmaI sites (position 3384 in cDNA) of pD102. The resulting clone, pHA3-17, rescued *lf3-5* and *lf3-6* mutants with the same effectiveness as the unmodified clone. To create an HA-tagged *lf3-2* construct, the *lf3-2* DNA was used as template for PCR and an AatII–MluI fragment containing the *lf3-2* mutation was substituted for the same region in the WT tagged gene.

lf3-5 and WT cells were grown in 250–1,000 ml of M medium with vigorous aeration for flagellar isolation. Preparation of total cell proteins, isolation of flagella, and procedures for immunoblots using the ECL detection system (Amersham Biosciences) were performed as described previously (Tam and Lefebvre, 2002). Primary antibodies were 3F10 against HA (Roche Biochemicals); antibodies to FLA10 and different IFT proteins (provided by D. Cole, University of Idaho, Moscow, ID; provided by J. Rosenbaum, Yale University, New Haven, CT); DHC1b (provided by M. Porter, University of Minnesota, Minneapolis, MN); PF16 (provided by E. Smith, Dartmouth College, Hanover, NH); IC140 (provided by W. Sale, Emory University, Atlanta, GA); RIB43 (provided by R. Linck, University of Minnesota, Minneapolis, MN); MBO2 (Tam and Lefebvre, 2002); β-tubulin (provided by G. Piperno, Mount Sinai School of Medicine, New York, NY); and OEE1 (provided by B. Barry, University of Minnesota, St. Paul, MN). Secondary antibodies were a sheep anti–mouse or anti–rat POD (Roche Biochemicals) or a goat anti–rabbit HRP secondary antibody (Sigma-Aldrich). Procedures for immunofluorescence were performed as described previously (Tam and Lefebvre, 2002), except that the detection of IFT components was performed using secondary antibodies conjugated to the Alexa 488 fluorochrome and the Slowfade Light Antifade kit as the mounting medium (Molecular Probes). Similar localization of HA-LF3p could be detected with cells fixed in 4% formaldehyde before permeabilization in methanol.

Preparation of cytoplasmic extracts and sucrose density gradients

Cellular proteins from freshly grown cells were extracted either by freezing (in liquid nitrogen) and thawing five times in 150 mM NaCl, 50 mM Tris, pH 7.5, 50 mM NaF, 25 mM β-glycerophosphate, 1–2 mM sodium orthovanadate, 1/100 vol of a protease inhibitor cocktail (Sigma-Aldrich), or by incubating in the same buffer containing 0.2% NP-40 for 30 min at 4°C. Insoluble materials were removed by centrifugation and soluble fractions were concentrated with Centricon-10 columns (Millipore). About 6–12 mg of soluble proteins in 0.5 ml were fractionated on an 11-ml 5–20% sucrose density gradients (prepared a day before by layering 2.75 ml each of 20, 15, 10, and 5% sucrose in 10 mM Hepes, pH 7.5) in a SWTi41 rotor for 12 h at 38,000 rpm. 0.46-ml fractions were drawn from the top of the gradients and subsequently analyzed by SDS-PAGE and immunoblotting. A gradient for sedimentation standards was included in every experiment.

We thank Dr. Carolyn Silflow, Dr. Mary Porter, Dr. Nedra Wilson, and Nancy Haas for helpful comments on the manuscript.

This work was supported by the National Institutes of Health (NIH) grant GM34437 to P.A. Lefebvre. L.-W. Tam was supported in part by an NIH postdoctoral fellowship and by National Science Foundation research training grant DIR-9113444.

Submitted: 22 July 2003
Accepted: 9 September 2003

References

Afzelius, B.A., G. Gargani, and C. Romano. 1985. Abnormal length of cilia as a possible cause of defective mucociliary clearance. *Eur. J. Respir. Dis.* 66:173–180.

Asleson, C.M., and P.A. Lefebvre. 1998. Genetic analysis of flagellar length control in *Chlamydomonas reinhardtii*: a new long-flagella locus and extragenic suppressor mutations. *Genetics.* 148:693–702.

Barsel, S.E., D.E. Wexler, and P.A. Lefebvre. 1988. Genetic analysis of long-flagella mutants of *Chlamydomonas reinhardtii. Genetics.* 118:637–648.

Berman, S.A., N.F. Wilson, N.A. Haas, and P.A. Lefebvre. 2003. A novel MAP ki-

nase regulates flagellar length in *Chlamydomonas*. *Curr. Biol.* 13:1145–1149.
Brazelton, W.J., C.D. Amundsen, C.D. Silflow, and P.A. Lefebvre. 2001. The *bld1* mutation identifies the *Chlamydomonas osm-6* homolog as a gene required for flagellar assembly. *Curr. Biol.* 11:1591–1594.
Cole, D.G. 2003. The intraflagellar transport machinery of *Chlamydomonas reinhardtii*. *Traffic.* 4:435–442.
Cole, D.G., D.R. Diener, A.L. Himelblau, P.L. Beech, J.C. Fuster, and J.L. Rosenbaum. 1998. *Chlamydomonas* kinesin-II-dependent intraflagellar transport (IFT): IFT particles contain proteins required for ciliary assembly in *Caenorhabditis elegans* sensory neurons. *J. Cell Biol.* 141:993–1008.
Deane, J.A., D.G. Cole, E.S. Seeley, D.R. Diener, and J.L. Rosenbaum. 2001. Localization of intraflagellar transport protein IFT52 identifies basal body transitional fibers as the docking site for IFT particles. *Curr. Biol.* 11:1586–1590.
Debuchy, R., S. Purton, and J.D. Rochaix. 1989. The argininosuccinate lyase gene of *Chlamydomonas reinhardtii*: an important tool for nuclear transformation and for correlating the genetic and molecular maps of the *ARG7* locus. *EMBO J.* 8:2803–2809.
Finst, R.J., P.J. Kim, E.R. Griffis, and L.M. Quarmby. 2000. Fa1p is a 171 kDa protein essential for axonemal microtubule severing in *Chlamydomonas*. *J. Cell Sci.* 113:1963–1971.
Gaffal, K.P. 1988. The basal body-root complex of *Chlamydomonas reinhardtii* during mitosis. *Protoplasm.* 143:118–129.
Harris, E.H. 1989. The *Chlamydomonas* Sourcebook. Academic Press, Inc., San Diego, CA. 780 pp.
Huang, B., M.R. Rifkin, and D.J. Luck. 1977. Temperature-sensitive mutations affecting flagellar assembly and function in *Chlamydomonas reinhardtii*. *J. Cell Biol.* 72:67–85.
Huang, B., Z. Ramanis, S.K. Dutcher, and D.J. Luck. 1982. Uniflagellar mutants of *Chlamydomonas*: evidence for the role of basal bodies in transmission of positional information. *Cell.* 29:745–753.
Iomini, C., V. Babaev-Khaimov, M. Sassaroli, and G. Piperno. 2001. Protein particles in *Chlamydomonas* flagella undergo a transport cycle consisting of four phases. *J. Cell Biol.* 153:13–24.
Jarvik, J.W., and B. Chojnacki. 1985. Flagellar morphology in stumpy-flagella mutants of *Chlamydomonas reinhardtii*. *J. Protozool.* 32:649–656.
Jarvik, J.W., F.D. Reinhardt, M.R. Kuchka, and S.A. Adler. 1984. Altered flagellar size control in *shf-1* short flagella mutants of *Chlamydomonas reinhardtii*. *J. Protozool.* 31:100–104.
Kozminski, K.G., K.A. Johnson, P. Forscher, and J.L. Rosenbaum. 1993. A motility in the eukaryotic flagellum unrelated to flagellar beating. *Proc. Natl. Acad. Sci. USA.* 90:5519–5523.
Kozminski, K.G., P.L. Beech, and J.L. Rosenbaum. 1995. The *Chlamydomonas* kinesin-like protein FLA10 is involved in motility associated with the flagellar membrane. *J. Cell Biol.* 131:1517–1527.
Kuchka, M.R., and J.W. Jarvik. 1987. Short-flagella mutants of *Chlamydomonas reinhardtii*. *Genetics.* 115:685–691.
Levy, E.M. 1974. Flagellar elongation: an example of controlled growth. *J. Theor. Biol.* 43:133–149.
Marshall, W.F., and J.L. Rosenbaum. 2001. Intraflagellar transport balances continuous turnover of outer doublet microtubules: implications for flagellar length control. *J. Cell Biol.* 155:405–414.
Matsuura, K., P.A. Lefebvre, R. Kamiya, and M. Hirono. 2002. Kinesin-II is not essential for mitosis and cell growth in *Chlamydomonas*. *Cell Motil. Cytoskeleton.* 52:195–201.
McVittie, A. 1972. Flagellum mutants of *Chlamydomonas reinhardii*. *J. Gen. Microbiol.* 71:525–540.
Niggemann, B., A. Muller, A. Nolte, N. Schnoy, and U. Wahn. 1992. Abnormal length of cilia–a cause of primary ciliary dyskinesia–a case report. *Eur. J. Pediatr.* 151:73–75.
Norrander, J.M., R.W. Linck, and R.E. Stephens. 1995. Transcriptional control of tektin A mRNA correlates with cilia development and length determination during sea urchin embryogenesis. *Development.* 121:1615–1623.
Orozco, J.T., K.P. Wedaman, D. Signor, H. Brown, L. Rose, and J.M. Scholey. 1999. Movement of motor and cargo along cilia. *Nature.* 398:674.
Pazour, G.J., C.G. Wilkerson, and G.B. Witman. 1998. A dynein light chain is essential for the retrograde particle movement of intraflagellar transport (IFT). *J. Cell Biol.* 141:979–992.
Pazour, G.J., B.L. Dickert, and G.B. Witman. 1999. The DHC1b (DHC2) isoform of cytoplasmic dynein is required for flagellar assembly. *J. Cell Biol.* 144:473–481.
Pazour, G.J., B.L. Dickert, Y. Vucica, E.S. Seeley, J.L. Rosenbaum, G.B. Witman, and D.G. Cole. 2000. *Chlamydomonas IFT88* and its mouse homologue, polycystic kidney disease gene *Tg737*, are required for assembly of cilia and flagella. *J. Cell Biol.* 151:709–718.
Perrone, C.A., D. Tritschler, P. Taulman, R. Bower, B.K. Yoder, and M.E. Porter. 2003. A novel dynein light intermediate chain colocalizes with the retrograde motor for intraflagellar transport at sites of axoneme assembly in *Chlamydomonas* and mammalian cells. *Mol. Biol. Cell.* 14:2041–2056.
Piperno, G., E. Siuda, S. Henderson, M. Segil, H. Vaananen, and M. Sassaroli. 1998. Distinct mutants of retrograde intraflagellar transport (IFT) share similar morphological and molecular defects. *J. Cell Biol.* 143:1591–1601.
Porter, M.E., R. Bower, J.A. Knott, P. Byrd, and W. Dentler. 1999. Cytoplasmic dynein heavy chain 1b is required for flagellar assembly in *Chlamydomonas*. *Mol. Biol. Cell.* 10:693–712.
Rautiainen, M., J. Nuutinen, and Y. Collan. 1991. Short nasal respiratory cilia and impaired mucociliary function. *Eur. Arch. Otorhinolaryngol.* 248:271–274.
Rechsteiner, M., and S.W. Rogers. 1996. PEST sequences and regulation by proteolysis. *Trends Biochem. Sci.* 21:267–271.
Rosenbaum, J.L., J.E. Moulder, and D.L. Ringo. 1969. Flagellar elongation and shortening in *Chlamydomonas*. The use of cycloheximide and colchicine to work the synthesis and assembly of flagellar proteins. *J. Cell Biol.* 41:600–619.
Rosenbaum, J.L., and G.B. Witman. 2002. Intraflagellar transport. *Nat. Rev. Mol. Cell Biol.* 3:813–825.
Sambrook, J., E.F. Fritsch, and T. Maniatis. 1989. Molecular Cloning: A Laboratory Manual. Cold Spring Harbor Laboratory, Cold Spring Harbor, NY. 7.43–7.45; 13.39–13.41.
Silflow, C.D., M. LaVoie, L.-W. Tam, S. Tousey, M. Sanders, W. Wu, M. Borodovsky, and P.A. Lefebvre. 2001. The Vfl1 protein in *Chlamydomonas* localizes in a rotationally asymmetric pattern at the distal ends of the basal bodies. *J. Cell Biol.* 153:63–74.
Tam, L.-W., and P.A. Lefebvre. 1993. Cloning of flagellar genes in *Chlamydomonas reinhardtii* by DNA insertional mutagenesis. *Genetics.* 135:375–384.
Tam, L.-W., and P.A. Lefebvre. 2002. The *Chlamydomonas MBO2* locus encodes a conserved coiled-coil protein important for flagellar waveform conversion. *Cell Motil. Cytoskeleton.* 51:197–212.
Tuxhorn, J., T. Daise, and W.L. Dentler. 1998. Regulation of flagellar length in *Chlamydomonas*. *Cell Motil. Cytoskeleton.* 40:133–146.
Walther, Z., M. Vashishtha, and J.L. Hall. 1994. The *Chlamydomonas FLA10* gene encodes a novel kinesin-homologous protein. *J. Cell Biol.* 126:175–188.
Wilkerson, C.G., S.M. King, and G.B. Witman. 1994. Molecular analysis of the gamma heavy chain of *Chlamydomonas* flagellar outer-arm dynein. *J. Cell Sci.* 107:497–506.